

**ANALYSIS OF BREAKTHROUGH PROFILES BASED ON GAMMA-RAY  
EMISSION ALONG LOADED PACKED BED COLUMNS:  
COMPARATIVE EVALUATION OF IONSIV® IE-911 AND  
CHABAZITE ZEOLITE FOR THE REMOVAL OF  
RADIOSTRONTIUM AND CESIUM FROM GROUNDWATER**

S. M. DePaoli, D. T. Bostick, and A. J. Lucero

Chemical Technology Division

Oak Ridge National Laboratory\*

P.O. Box 2008

Oak Ridge, Tennessee 37831-6201

A gamma counting system has been assembled that can profile the breakthrough fronts of gamma-emitting radioisotopes longitudinally and axially along a loaded column. This profiling technique has been particularly useful in column studies such as those performed with IONSIV® IE-911, a crystalline silicotitanate (CST) manufactured by UOP, in which unusually long operating times are required to observe cesium breakthrough in column effluent. The length of the mass transfer zone and extent of column saturation can be detected early in a column study by viewing the relative emission of gamma emitters along the length of the column. In this study, gamma scans were used to analyze loaded CST and zeolite columns used in the treatment of process wastewater simulant and actual groundwater. Results indicate good run-to-run reproducibility in acquiring the scans. The longitudinal gamma scans for both <sup>90</sup>Sr and <sup>137</sup>Cs conformed with breakthrough results reported on the basis of column effluent activity. Although not obvious from data obtained by monitoring effluent activity, the gamma scans indicated that both cesium and strontium in the saturated zone of the CST column are slowly displaced by the higher levels of groundwater cations and are then resorbed further down the column. This displacement phenomenon identified by gamma scans was verified using data from a zeolite column, in which both the gamma scan and column effluent data exhibited radionuclide displacement by groundwater cations. The gamma emission intensities from the CST column runs are used to quantitate and compare the distribution coefficient and loading capacity of <sup>137</sup>Cs on CST versus zeolite.

**INTRODUCTION**

Gamma scanning equipment was designed to allow the location of gamma emitters along loaded columns used to treat radioactively contaminated wastewaters. Several columns archived from tests of sorbent efficiency in the removal of <sup>90</sup>Sr and <sup>137</sup>Cs were scanned with the portable gamma system. These results were compared with standard column breakthrough data acquired by analyzing the radionuclide contents of column effluent fractions. In the first test, engineered CST was used to treat process wastewater simulant (refer to Table 1 for water composition). The column run lasted for 10 months, during which time

maximum  $^{90}\text{Sr}$  breakthrough in the column effluent did not exceed 28% and  $^{137}\text{Cs}$  was not observed in the effluent. In the case of cesium sorption on CST, an operating time of 17 years was estimated to observe complete breakthrough using the process wastewater feed. A second column test used CST to remove strontium and cesium from seep water collected from a burial ground located at Oak Ridge National Laboratory (ORNL). The seep water is contaminated with  $^{90}\text{Sr}$ ; however, cesium was added to the feed so that the efficiencies of the sorbents for cesium removal might also be observed. The feed, designated as Seep D water (Table 1), was treated under identical column conditions as the first study. Finally, the portable gamma system was used to scan a third archived column that contained the sorbent chabazite zeolite, and

Table 1  
Composition of Process Waste Treatment Plant (PWTP) Actual and Simulant  
Wastewater, Seep D Water, and Groundwater from Core Hole 8 Sump

Component	Concentration (mg/L)		
	PWTP, actual	PWTP, simulant	Seep D water <sup>a</sup>
$\text{Ca}^{2+}$	35–40	45	76
$^{137}\text{Cs}^+$	$9.4 \times 10^{-8}$ ( $3.0 \times 10^2 \text{ Bq/L}$ )	$3.4 \times 10^{-4}$ ( $1.12 \times 10^6 \text{ Bq/L}$ )	$3.4 \times 10^{-4}$ ( $1.12 \times 10^6 \text{ Bq/L}$ )
$\text{K}^+$	1–3	1.2	1.6
$\text{Mg}^{2+}$	7–8	8.8	9.1
$\text{Na}^+$	14–30	18.3	8.7
$\text{Sr}^{2+}$ (total)	0.1	0.1	0.1
$\text{Sr}^{2+}$ (rad.)	$5.3 \times 10^{-8}$ as $^{90}\text{Sr}$ ( $2.70 \times 10^2 \text{ Bq/L}$ )	$1.14 \times 10^{-6}$ as $^{85}\text{Sr}$ ( $1.0 \times 10^6 \text{ Bq/L}$ )	$5.33 \times 10^{-6}$ as $^{90}\text{Sr}$ ( $2.7 \times 10^4 \text{ Bq/L}$ )
pH	6.7–9	7–8	8

<sup>a</sup>Cesium was added to this wastewater in tracer levels.

had been used to treat Seep D water.

The breakthrough data, based on column effluent and gamma scan results, were compared and then used

to calculate the distribution and mass transfer coefficients of  $^{90}\text{Sr}$  and  $^{137}\text{Cs}$  in the various column runs.

## EXPERIMENTAL METHODS

### Small Column Setup

Column testing was used to define the sorption characteristics of a ion exchanger under dynamic flow conditions. The initial dimensions of a sorbent column were selected primarily on the basis of the diameter of the average sorbent particle.<sup>1</sup> Results of previous small-column experiments were used to modify initial estimates to allow for practical limitations in preparing large volumes of simulant and in limiting the duration of the column test. Although the optimum column diameter should be at least 40 times greater than the average particle diameter (typically 0.059 cm, or 30 mesh), a factor of 20 was considered adequate for testing. A column diameter of 1 cm meets these requirements and was used for comparative testing of the sorbents. The optimum length of the column should be greater than or equal to four times the column diameter; the typical column aspect ratio for testing is between 4 and 5. Approximately 2–4 g (depending on the exchanger) of preconditioned sorbent was packed in the 1-cm-ID columns, resulting in a bed volume of 4–5 mL.

Column preparation was done, in each case, by slowly adding conditioned sorbent from a weighed container to a 1-cm column containing a known volume of water. The sorbent was added to a column bed depth of 4.8–5 cm, and the dry sorbent container was then reweighed to determine the amount of sorbent added to the column. Excess water above the column bed was collected and weighed. The difference between the initial water volume in the column and the volume of water displaced by the sorbent represented the pore volume of the sorbent column. The pore fraction was equivalent to the measured pore volume of the 1-cm column divided by the column volume, calculated on the basis of bed height.

A peristaltic pump was used to transfer the feed solution through a 0.45- $\mu\text{m}$  Supor<sup>TM</sup> filter membrane into the base of the sorbent column (Fig. 1). The flow rate of feed was maintained at about 1.2 mL/min, or 18 - 20 bed volumes (BV)/h. The feed was introduced at the bottom of the column to maximize contact of

the solution and sorbent within the column. An automatic fraction collector was used to collect the column effluent over 2- to 10-h periods (about 36 to 190 BV per fraction). Actual fraction volumes were determined by multiplying the value for the density of the feed stream (0.9965 g/mL) by the tared weight of the solution in the fraction. The radionuclide content of each fraction was determined, while aliquots of intermittent fractions were acidified and submitted for analysis by inductively coupled plasma mass spectroscopy to determine the cationic concentrations in the effluent.

### Gamma Scanning of Columns

Gamma scanning equipment was designed to determine the quantities and locations of gamma emitters along loaded columns used to treat Process Wastewater Treatment Plant (PWTP) simulant and actual seep water. This system is particularly useful for column tests in which the loading capacity of the sorbent for a given emitter is so large that unduly long operating times are required to observe the breakthrough of a species. In the case of cesium sorption on CST, an operating time of 17 years was estimated to observe complete breakthrough using the PWTP feed. The portable gamma counting system locates the position of the cesium mass transfer zone within the CST column and allows an accurate extrapolation of cesium breakthrough parameters based on limited column operation.

A lead-brick apparatus was used to hold the 1-cm-ID columns loaded in the previously described column experiments. The lead shielding was designed and constructed to enable a gamma scan of the column in longitudinal and axial increments. Figure 2 shows the design and measurements of the lead shielding. The column was inserted horizontally into the 1-in.-diam hole. A nominal 0.28-cm slit and several lead rings were used to select and moderate the gamma radiation from 0.25-in. lengths of the column surface. A

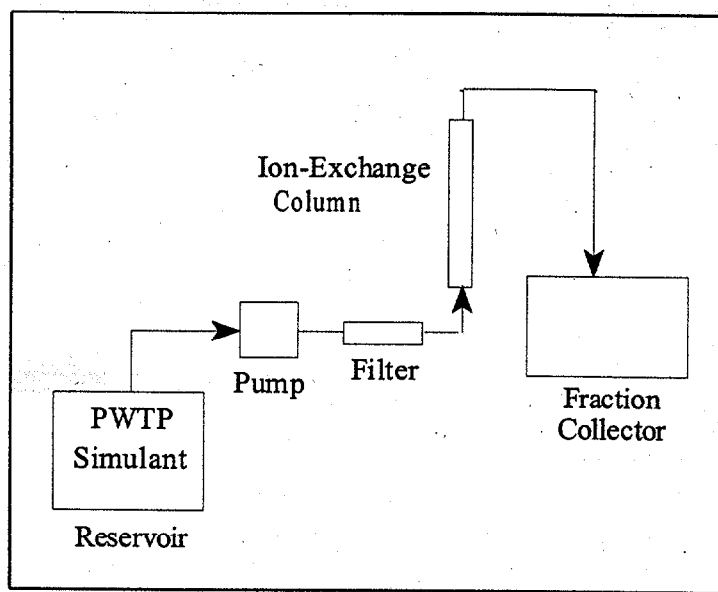


Fig. 1. Flow diagram for column test.

Lead Brick 1	Lead Brick 2
Quantity: 1	Quantity: 3
Plug	Assembly
Quantity: 4	

Fig. 2 Lead shielding apparatus for gamma scanning of columns.

metered push rod was used to index the gamma count rate with longitudinal column position, as the loaded column was pushed past the detector slit. A portable gamma spectroscopy system with a 3-in. high-purity germanium detector (NOMAD-PLUS, supplied by EG&G ORTEC, Oak Ridge, Tennessee) was used to acquire the gamma count rate along the column length; EG&G ORTEC Gamma Vision spectroscopy software was used for spectrum analysis and hardware control.

## RESULTS AND DISCUSSION

### Radionuclide Breakthrough Based on Column Effluent Results

#### *CST Treatment of Process Water Simulant*

The small-column test using the hydrogen form of IONSIV® IE-911 (Hydrogen-CST) to treat PWTP simulant was carried out over a period of 10 months; a total of 120,000 BV was processed during this time.

The CST selectivity of cesium over strontium is demonstrated in Fig. 3, which shows the beginning of strontium breakthrough. Cesium breakthrough was not observed, even up to 120,000 BV. The strontium breakthrough curve is very atypical, where  $C/C_0$  increases (as expected) up to 0.28, but then decreases, increases again, and subsequently decreases again, to approximately 0.15 at 120,000 BV. A complex mechanism for strontium sorption and ion exchange is obviously occurring, and while multicomponent sorption and desorption may account for some of these phenomena, perhaps the availability of sites within the sorbent is also changing during the diffusion process. A linear extrapolation of the breakthrough curve from the point at which the column test was terminated would give 50% breakthrough of strontium at 175,000 BV.

#### *CST Treatment of Actual Seep D Water*

Engineered Hydrogen-CST was again used in a column test, this time with a feed stream consisting of actual water from ORNL Seep D site located in the WAG 5 burial grounds. The composition of the Seep D water is shown in Table 1;  $^{90}\text{Sr}$  is present in the water, while the cesium was added only for observational

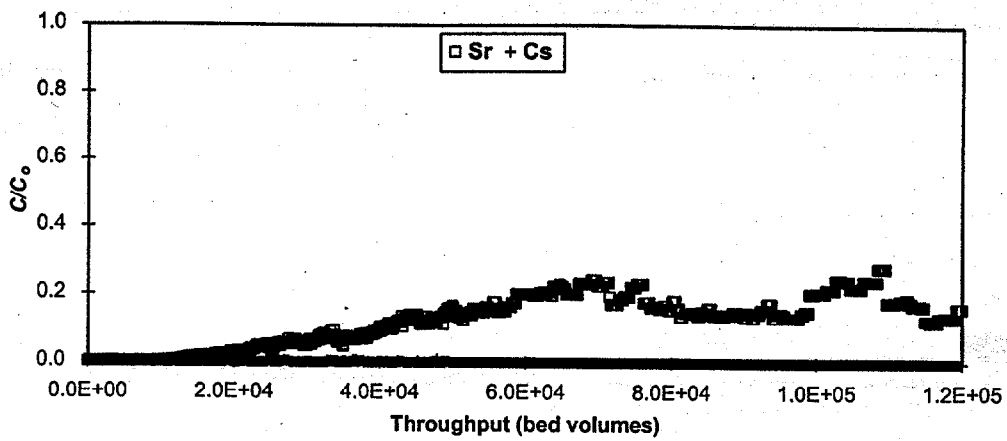


Fig. 3. Breakthrough of strontium and cesium on CST from PWTP simulant.

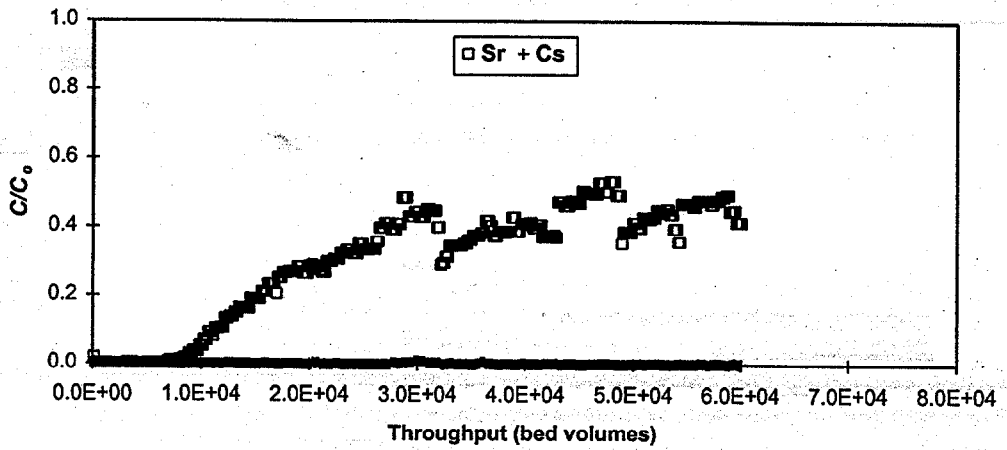


Fig. 4. Breakthrough of strontium and cesium on CST from Seep D water.

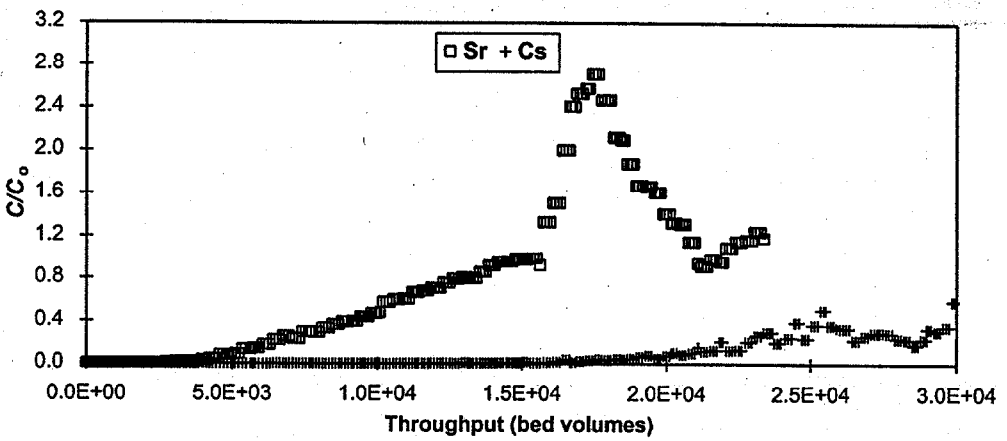


Fig. 5. Breakthrough of strontium and cesium on zeolite from Seep D water.

purposes. Note that the calcium concentration is almost twice that of the PWTP simulant column feed. Again, the CST selectivity of cesium over strontium is demonstrated in Fig. 4, which shows no cesium breakthrough, up through column test completion at 61,400 BV. The strontium breakthrough curve is very unusual, but similar to the strontium breakthrough for the PWTP column test (see Fig. 3).

### ***Zeolite Treatment of Actual Seep D Water***

A column test comparable to the CST/Seep D water column experiment was performed using chabazite zeolite with the Seep D water feed (Table 1). As mentioned before, this seep water contains  $^{90}\text{Sr}$ ; cesium was added simply for observational purposes. Figure 5 shows the breakthrough of strontium and cesium on zeolite in Seep D water. Incipient (1%) strontium breakthrough occurred at 2000 BV, 50% strontium breakthrough occurred at 10,100 BV. In most zeolite column studies reported in the literature, the run was terminated at this point and a strontium  $K_d$  was calculated on the basis of the quantity of strontium sorbed on the column to this point. However, continuation of the column run showed that sorbed strontium is not retained on the column; instead, it was displaced from the zeolite as the C/C<sub>o</sub> ratio increased above 1.0. By 22,000 BV, more than half the strontium originally sorbed onto the column was displaced from the zeolite by competing water cations. No cation displacement was observed from the comparable CST column test, even at a throughput of 60,000 BV seep water.

### **Radionuclide Breakthrough Based on Gamma Scanning Results.**

#### ***CST Treatment of Process Water Simulant***

Figure 6 shows the gamma scan profile of the CST column test using PWTP simulant feed. Approximately 300 meq of strontium and 0.3 meq of cesium per kilogram of CST had been sorbed onto the column when the test was terminated in February 1998. Accounting for the decay of  $^{85}\text{Sr}$ , 3  $\mu\text{Ci}$  of  $^{85}\text{Sr}$  and 13  $\mu\text{Ci}$  of  $^{137}\text{Cs}$  were present in the column when the scan was taken; the dose rate of the column was 50 mRem/h at contact.

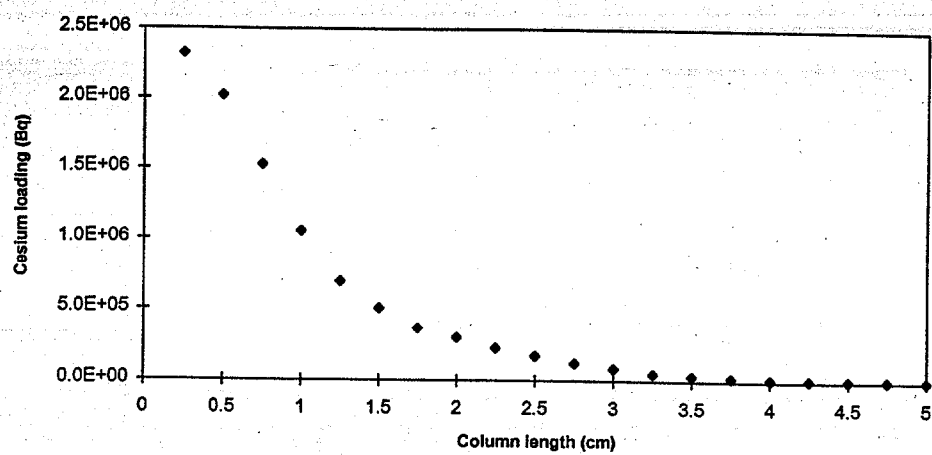


Fig. 6. Gamma scan of column showing cesium loading on Hydrogen-CST from PWTP simulant feed. (0 cm = column inlet).

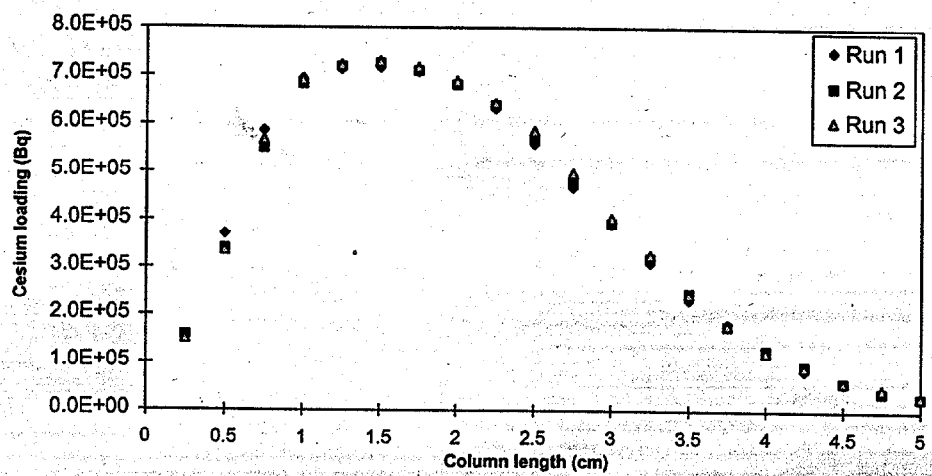


Fig. 7. Gamma scan of column showing cesium loading on Hydrogen-CST from Seep D water. (0 cm = column inlet).

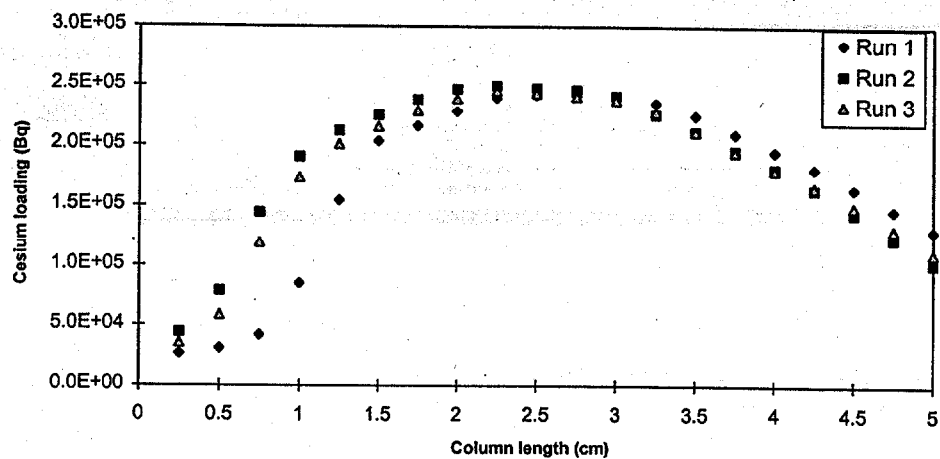


Fig. 8. Gamma scan of column showing cesium loading on zeolite from Seep D water. (0 cm = column inlet).

Each data point in the figure represents the count rate of 0.25-cm lengths, starting from the head of the column. The  $^{137}\text{Cs}$  profile indicates that the mass transfer zone was ~1 cm long; therefore, less than 25% of the sorbent bed was saturated with cesium. The gamma scan data were used to calculate the distribution coefficient ( $K_d$ ) and loading capacity of  $^{137}\text{Cs}$  on CST. The  $K_d$  for cesium removal from process water was 850,000 (L/kg) on CST as compared with 90,000 (L/kg) on zeolite.<sup>2</sup> The calculated CST loading capacity, based on the gamma scan results, indicated that the point of 50% cesium saturation was 2.1 meq/kg. Strontium detection was hampered by the lower-energy gamma emission (514 keV) that was moderated by the CST and shielding from the glass column, as well as by the interference of a secondary  $^{137}\text{Cs}$  emission at this same energy. Therefore, the signal-to-noise ratio in  $^{85}\text{Sr}$  detection was limited relative to that of  $^{137}\text{Cs}$ . Nonetheless, the  $^{85}\text{Sr}$  profile indicates that the strontium mass transfer zone extended nearly the full length of the column (3.8 cm), suggesting full utilization of the column bed. This value conforms to a C/C<sub>o</sub> of 15-20%, which was determined by the analysis of column effluent.

#### ***CST Treatment of Actual Seep D Water***

Figure 7 illustrates radionuclide loading profiles on CST using Seep D water as the column feed. The excellent reproducibility in gamma profiles of the column in triplicate scanning runs is evident in this figure. The cesium  $K_d$  in the Seep D water matrix was 150,000 (L/kg), indicating a reduction in cesium loading capacity on CST due to a higher calcium concentration (i.e. twice that present in PWTP simulant).

#### ***Zeolite Treatment of Actual Seep D Water***

Gamma scan results also identified significant displacement of radionuclides in the upstream portion of the zeolite column (Fig. 8), and, to a much smaller extent, from the CST column (Fig. 7) during the treatment of actual seep water. Although effluent activity indicated that strontium was desorbed from the zeolite, the gamma scan indicates that both cesium and strontium in the saturated zone of the zeolite column were

displaced by the higher levels of water cations and were then resorbed farther down the column. The cesium  $K_d$  in the Seep D water matrix was a factor of 3 lower on the zeolite (50,000 L/kg) than that observed with CST in the same water matrix.

The gamma scan data were also used to predict the breakthrough profiles for cesium. The scans provide a profile within the column, and knowledge of the time dependency of these internal profiles allows typical column breakthrough profiles to be generated. Figure 9 shows the actual effluent analysis breakthrough of cesium on chabazite zeolite. The second set of data points, "gamma scan analysis", shows the projected breakthrough based on the gamma analysis of the column. Validation of the use of the gamma scans to predict breakthrough is seen in the excellent agreement of these two sets of data. This treatment, along with the distribution coefficients obtained through the gamma data, was used to predict the breakthrough curves for cesium on CST (see Figs. 10 and 11). A prediction method (Rosen model) was also employed to determine mass transfer coefficients for the CST in the given water matrices. This method is discussed in the following section.

### Calculation of Column Mass Transfer Coefficients

All column experimental data were fit to the Rosen solution<sup>3</sup>, which is valid for long-bed systems.<sup>4</sup> Both the film- and the particle-side resistances to mass transfer are accounted for in the model. Rosen began with two basic assumptions: (1) the diffusional parameters for both the film and particle are independent of concentration and position in the column, and (2) adsorption of the solute(s) can be represented by a linear isotherm. Thus the linear representation of equilibrium is written as

$$q_s = K_d c, \quad (1)$$

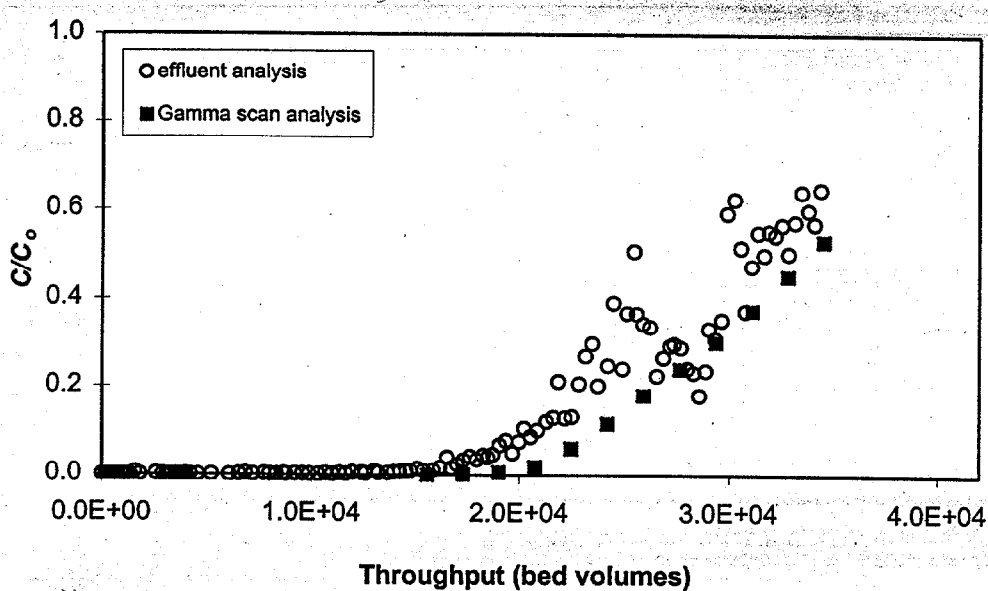


Fig. 9. Cesium breakthrough on chabazite zeolite, determined by effluent analysis and gamma scans of column. Test conditions: 2.3 g chabazite zeolite; 1-cm-ID column; bed length, 4.8 cm; flow rate of Seep D water 1.2 mL/min.

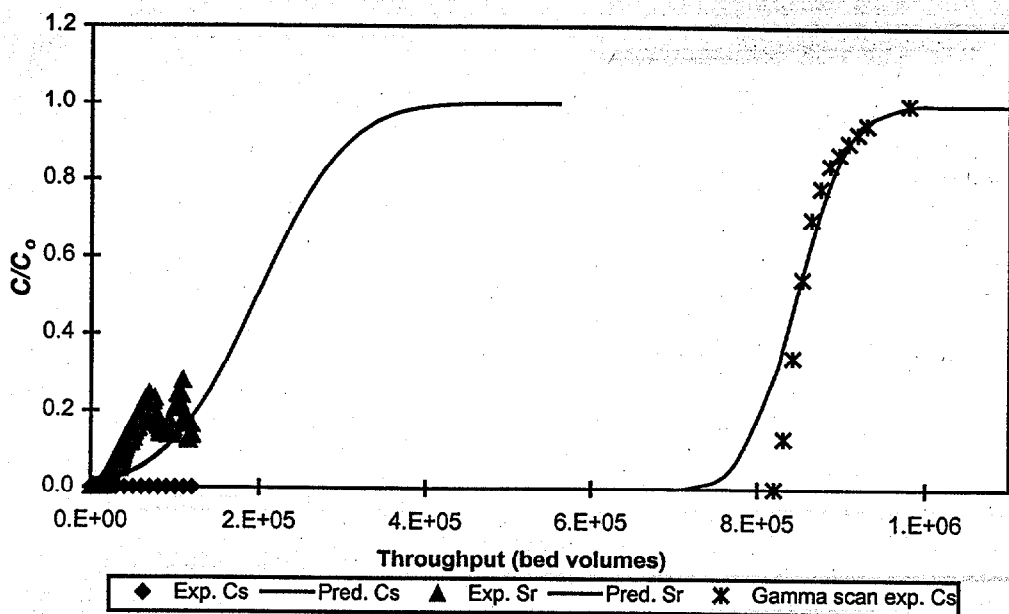


Fig. 10. Experimental and predicted breakthrough of strontium and cesium on Hydrogen-CST in PWTP simulant. Test conditions: 3.81 g Hydrogen-CST; 1-cm-ID column; bed length, 4.85 cm; PWTP simulant flow rate, 1.2 mL/min.

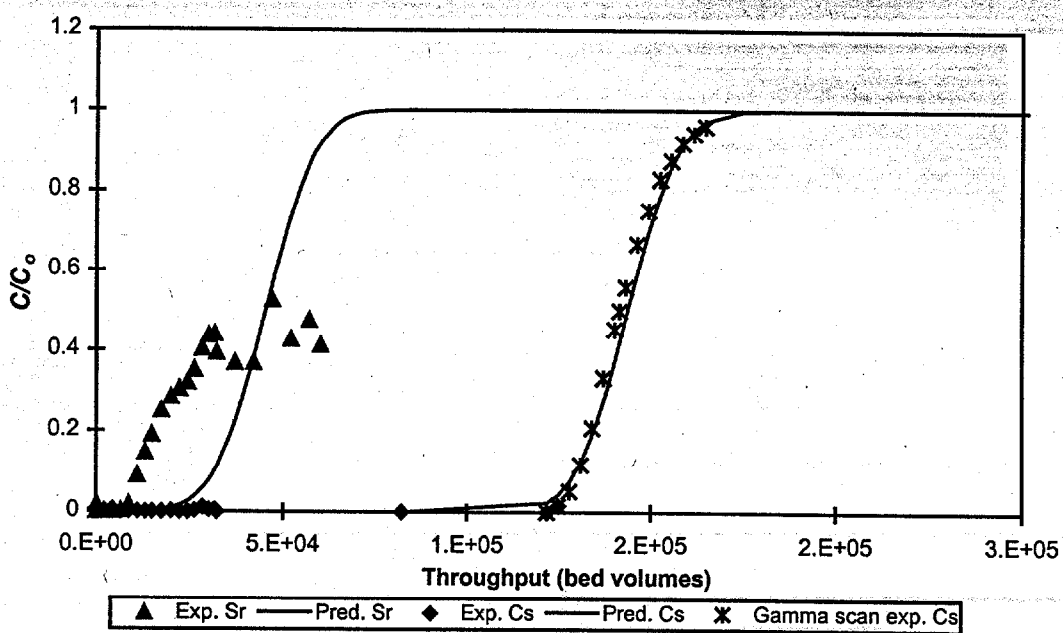


Fig. 11. Experimental and predicted breakthrough of strontium and cesium on Hydrogen-CST in Seep D water. Test conditions: 3.85 g of Hydrogen-CST; 1-cm-ID column; 5.2-cm bed length; feed flow rate, 1.2 mL/min.

where

$q_s$  = the concentration on the solid, meq/kg;  
 $K_d$  = the equilibrium constant, or distribution coefficient, L/kg;  
 $c$  = the concentration in the liquid, meq/L.

Based on these assumptions, Rosen presented an analytic solution to the mass balance equation

$$\nu \frac{\partial c}{\partial z} + \frac{\partial c}{\partial t} = -\frac{1}{m} \frac{\partial q}{\partial t} \quad (2)$$

as:

$$\frac{C}{C_0} = \frac{1}{2} \left( 1 + \operatorname{erf} \left( \frac{(3/2)X}{2\sqrt{\nu}t} \right) \right), \quad (3)$$

where

$$X = \frac{3 D_p K_d \rho_s (1 - \varepsilon) Z}{\varepsilon U_z R^2} \quad (\text{bed-length parameter}), \quad (4)$$

$$\nu = \frac{D_p K_d \rho_s}{R k_f} \quad (\text{film-resistance parameter}), \quad (5)$$

and

$$Y = \frac{2 D_p}{R^2} - \left( t - \frac{Z}{U_z} \right) \quad (\text{contact-time parameter}). \quad (6)$$

The variables in the above equations are defined as follows:

$D_p$  = effective diffusivity in the particle,  $\text{cm}^2/\text{s}$ ;  
 $R$  = radius of the particle, cm;  
 $U_z$  = interstitial liquid velocity,  $\text{cm/s}$ ;  
 $t$  = time, s;  
 $k_f$  = film mass transfer coefficient,  $\text{cm/s}$ ;  
 $C$  = concentration of solute at time  $t$ , meq/L;  
 $C_0$  = concentration of solute in feed, meq/L;  
 $\varepsilon$  = void fraction in column;  
 $Z$  = bed length, cm;  
 $\rho_s$  = density of solid, kg/L.

This solution was used to predict strontium and cesium breakthrough profiles for the CST column

experiments. All the measured material and column variables (exchanger weights, bed length, flow rates, etc.) used in the predictions are summarized in Table 2.

The validity of the simplified Rosen solution requires that the bed-length parameter,  $X$ , be greater than 40.<sup>5</sup> Material-specific, adjustable parameters needed to complete the above solution include the effective diffusivity in the particle and the film mass transfer coefficient. In order for  $X$  to be greater than 40, the effective diffusivities must exceed a given value. An effective particle diffusivity of  $2.7 \times 10^{-7} \text{ cm}^2/\text{s}$  was assumed for cesium diffusing into the particle. This assumption is supported by researchers at Texas A&M,<sup>6</sup> who have calculated and verified this effective diffusivity for cesium in CST. Using this value,  $X$  exceeds 40. An effective diffusivity of  $5.0 \times 10^{-5} \text{ cm}^2/\text{s}$  was assumed for strontium.<sup>7</sup>

Table 2  
Summary of Variables in Column Experiments

Variable	PWTP simulant feed		Seep D water feed	
	Chabazite zeolite	Hydrogen-CST	Chabazite zeolite	Hydrogen-CST
Exchanger weight, g	2.13	3.81	2.30	3.85
Particle diameter, $\mu\text{m}$	484	420	484	420
Column diameter, cm	1.0	1.0	1.0	1.0
Bed length, cm	4.9	4.85	4.8	5.2
Bed volume, mL	3.85	3.81	3.77	4.08
Flow rate, mL/min	1.28	1.21	1.25	1.2
Column void fraction	0.48	0.47	0.48	0.47

The film mass-transfer coefficients for each cationic species were calculated from empirical relationships presented in *The Chemical Engineers' Handbook*, by Perry and Chilton,<sup>8</sup> as

$$k_f = \frac{10.9 V (1 - \varepsilon)}{d_p a_p} \left[ \frac{D_f}{d_p V} \right]^{0.51} \left( \frac{D_f \rho_f}{\mu} \right)^{0.16}, \quad (7)$$

or

$$k_f = \frac{4.367 (1 - \varepsilon) (D_f V)^{0.5}}{d_p^{1.5} a_p}, \quad (8)$$

where

$V$  = volumetric flow rate,  $\text{cm}^3/\text{s}$ ;

$D_f$  = fluid-phase diffusivity,  $\text{cm}^2/\text{s}$ ;

$d_p$  = diameter of particle,  $\text{cm}$ ;

$a_p$  = outer surface area of particles per unit volume of contacting system,  $6(1-\varepsilon)/d_p$ ,  $\text{cm}^{-1}$ ;

$\mu$  = fluid viscosity, poises.

The coefficients were then adjusted to predict the actual experimental data more accurately. For strontium, the addition of a term to account for longitudinal dispersion was necessary.<sup>8</sup> For cesium, the film coefficient had to be increased to account for the slower mass transfer mechanism. Table 3 summarizes the calculated film mass-transfer coefficients for each experiment, and Table 4 gives the liquid diffusivities for each cation as calculated from the Nernst equation.<sup>9</sup>

Figures 10 and 11 show this prediction of the experimental data. Prediction of the breakthrough curves for strontium is dependent on the distribution coefficient used. A median value was used in each case. Because strontium had such an irregular breakthrough curve on CST, the model was unable to predict the experimental data satisfactorily. For cesium, the model predicted the gamma analysis-generated data closely.

Table 3  
Mass-Transfer Coefficients Calculated for Column Breakthrough Curve Predictions

Cation	Film mass-transfer coefficients ( $k_f \times 10^{-3}$ , $\text{cm}^2/\text{s}$ )			
	PWTP simulant feed stream		Seep D feed stream	
	Zeolite	Hydrogen-CST	Zeolite	Hydrogen-CST
$\text{Cs}^+$	1.26	1.28	1.68	1.23
$\text{Sr}^{2+}$	0.5	0.35	0.7	0.35

Table 4  
Liquid Diffusivities for Cesium and Strontium  
as Calculated by the Nernst Equation

Cation	Liquid diffusivity, $D_p$ , $\text{cm}/\text{s}$
$\text{Cs}^+$	$1.5 \times 10^{-5}$
$\text{Sr}^{2+}$	$1.02 \times 10^{-5}$

## CONCLUSIONS

The gamma scanning system described here is particularly useful for column tests in which the loading capacity of the sorbent for a given emitter is so large that unduly long operating times are required to observe cation breakthrough. In addition to determining the relative count rates of  $^{85}\text{Sr}$  and  $^{137}\text{Cs}$ , the quantities of these nuclides on the sorbent at a given column position could be quantified by determining spectrometer counting efficiency using a gamma-emitter standard. To accomplish this, both CST and zeolite sorbents could be slurried with a known volume of a mixed radionuclide gamma-ray reference standard, dried, and packed into a 1-cm glass column and counted under identical geometric configurations. A mass balance

could then be made between the known amounts of strontium and cesium loaded on the wastewater columns versus those measured by gamma emission to verify spectroscopic results.

Figure 6 shows a gamma scan profile of the CST column test using PWTP simulant feed. Approximately 300 meq of strontium and 0.3 meq of cesium per kilogram of CST had been sorbed onto the column when the run was terminated in February 1998. Accounting for the decay of  $^{85}\text{Sr}$ , 3 microcuries of  $^{85}\text{Sr}$  and 13 microcuries of  $^{137}\text{Cs}$  were present in the column when the scan was taken; the dose rate of the column was 50 mR/h at contact.

Each data point in the figure represents the count rate of 0.25-cm lengths, starting from the head of the column. The  $^{137}\text{Cs}$  profile indicates that the mass transfer zone was ~1 cm long; therefore, less than 25% of the sorbent bed was saturated with cesium. The gamma scan data were used to calculate the distribution coefficient ( $K_d$ ) and the loading capacity of  $^{137}\text{Cs}$  on CST. The  $K_d$  for cesium removal from process water was 850,000 (L/kg) on CST as compared with 90,000 (L/kg) on zeolite in PWTP simulant, and 150,000 L/kg for cesium removal from Seep D water by CST and 50,000 (L/kg) for chabazite zeolite. The calculated CST loading capacity, based on the gamma scan results, indicated that the point of 50% cesium saturation was 2.1 meq/kg. Strontium detection was hampered by the lower-energy gamma emission (514 keV) that is moderated by the CST and shielding from the glass column, as well as by the interference of a secondary  $^{137}\text{Cs}$  emission at this same energy. Therefore, the signal-to-noise ratio in  $^{85}\text{Sr}$  detection was limited relative to that of  $^{137}\text{Cs}$ . Nonetheless, the  $^{85}\text{Sr}$  profile indicates that the strontium mass transfer zone extended nearly the full length of the column (3.8 cm), suggesting full utilization of the column bed. This value conforms to a C/C<sub>o</sub> of 15-20% as determined by the analysis of column effluent.

Figure 8 illustrates radionuclide loading profiles on CST using Seep D water as the column feed. The excellent reproducibility in gamma profiles of the column in triplicate scanning runs is evident in this figure. The cesium  $K_d$  in the Seep D water matrix was 150,000 (L/kg), indicating a reduction in cesium loading capacity on CST at a calcium concentration of twice that present in the PWTP process simulant.

Gamma scan results also identified significant displacement of radionuclides in the upstream portion of

the zeolite column (Fig. 8) and, to a much smaller extent, from the CST column (Fig. 7) during the treatment of actual seep water. Although effluent activity indicated that strontium was desorbed from the zeolite, the gamma scan indicated that both cesium and strontium in the saturated zone of the zeolite column were displaced by the higher levels of water cations and were resorbed farther down the column. The cesium  $K_d$  in the Seep D water matrix was a factor of 3 lower on zeolite (50,000 L/kg) than that observed for CST in the same water matrix.

The gamma scans were successfully used to predict cesium breakthrough as demonstrated by Fig. 9. Figures 10 and 11 show the extrapolated breakthrough profiles for cesium based on the distribution coefficients calculated using gamma scan results; these data were then fit to the Rosen model to give film mass transfer coefficients and modeled breakthrough curves.

## REFERENCES

1. J. F. Relyea, "Theoretical and Experimental Considerations for Use of the Column Method for Determining Retardation Factors," *Radioactive Waste Management Nuclear Fuel Cycle*, 3, 151 (1982).
2. D. T. Bostick, S. M. DePaoli, and B. Guo, *Evaluation of Improved Techniques for the Removal of Fission Products from Process Wastewater and Groundwater: FY 1998 Status*, Report ORNL/TM-13689, Oak Ridge National Laboratory, Oak Ridge, Tennessee, September 1999.
3. J. B. Rosen, "Kinetics of a Fixed Bed System for Solid Diffusion into Spherical Particles," *J. Chem. Phys.* 20 (March 1932).
4. J. J. Perona, A. C. Coroneos, T. E. Kent, and S. A. Richardson, "A Simple Model for Strontium Breakthrough on Zeolite Columns," presented at the Eighth Symposium on Separation Science and Technology for Energy Applications, Gatlinburg, Tennessee, Oct. 23-27, 1993.
5. A. L. Hines and R. N. Maddox, *Mass Transfer Fundamentals and Applications*, Prentice-Hall, Inc., Englewood Cliffs, New Jersey, 1985.
6. M. E. Huckman and R. G. Anthony, paper presented at the Tenth Symposium on Separation Science and Technology, Gatlinburg, Tennessee, Oct. 20-24, 1997.
7. S. M. Robinson, W. D. Arnold, Jr., and C. H. Byers, *Multicomponent Liquid Ion Exchange with Chabazite Zeolites*, Report ORNL/TM-12403, Oak Ridge National Laboratory, Oak Ridge, Tennessee, October 1993.
8. R. H. Perry and C. H. Chilton, Eds., *Chemical Engineers' Handbook*, 5th ed., McGraw-Hill Book Co., New York, 1973.
9. R. A. Robinson and R. H. Stokes, *Electrolyte Solutions*, 2nd ed., Butterworths, London, 1959.